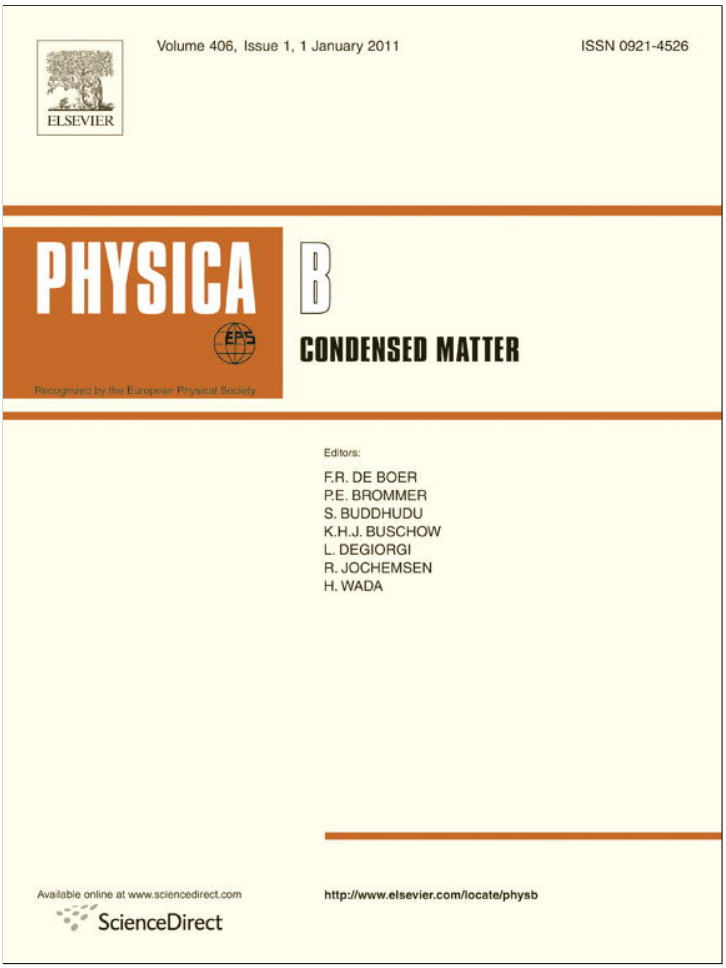

Physica B 406 (2011) 19–23

Contents lists available at ScienceDirect

Physica B

journal homepage: www.elsevier.com/locate/physb

Room temperature ferromagnetic pure ZnO

Qingyu Xu [a,*], Zheng Wen [b], Liguo Xu [c], Jinlong Gao [d], Di Wu [b], Kai Shen [c], Teng Qiu [a], Shaolong Tang [d], Mingxiang Xu [a]

[a] Department of Physics, Southeast University, Nanjing 211189, China
[b] Department of Materials Science and Engineering, Nanjing University, Nanjing 210008, China
[c] School of Materials Science and Technology, Nanjing University of Aeronautics and Astronautics, Nanjing 210016, China
[d] Department of Physics, Nanjing University, Nanjing 210008, China

ARTICLE INFO

Article history:
Received 22 July 2010
Received in revised form
18 September 2010
Accepted 30 September 2010

Keywords:
Diluted magnetic semiconductor
ZnO
Oxygen vacancies
Ferromagnetism

ABSTRACT

Pure ZnO films were prepared by pulsed laser deposition on oxidized Si substrates under different oxygen pressure and substrate temperature. Clear room temperature ferromagnetism has been observed in the ZnO film prepared under high vacuum and room temperature. The observation of anomalous Hall effect confirms the intrinsic nature of the ferromagnetism. The photoluminescence and X-ray photoelectron spectroscopy spectra show the high concentration of oxygen vacancies in the ferromagnetic ZnO film. Our results clearly demonstrate the ferromagnetic contribution of the oxygen vacancies mediated by the spin polarized electrons hopping between discrete states in pure ZnO.

1. Introduction

Diluted magnetic semiconductors (DMS) with simultaneous control of charge and spin, have attracted much attention due to their important applications in semiconductor spintronics [1,2]. Dietl et al. [3] theoretically predicted the possible DMS with T_c higher than room temperature (RT) in 5% Mn-doped p-type conductive ZnO and GaN. Interestingly, RT ferromagnetism has also been observed in pure ZnO [4–6]. In our previous study and Khalid et al.'s [5] work, Zn vacancies were attributed to the ferromagnetic origins in ZnO [4]. Banerjee et al. [6], Xing et al. [7], and Sundaresan et al. [8] attributed the RT ferromagnetism to the O vacancies. However, Hong et al. [9] concluded that the RT ferromagnetism does not stem from O vacancies but from the defects on Zn sites. Yi et al. [10] observed the RT ferromagnetism in incompletely oxidized ZnO nanowires and films, and the ferromagnetism was attributed to the Zn nanoclusters embedded in a ZnO matrix. The theoretical calculations by Zuo et al. [11] have pointed out that both O interstitial and Zn vacancy may induce ferromagnetism in ZnO. Wang et al. [12] pointed out that the ferromagnetism in ZnO is due to Zn vacancies instead of O vacancies. Thus the origin of the ferromagnetism in nonmagnetic doped ZnO is still unclear, and the magnetic role of the defects in ZnO needs further study. In this work, we concentrate on the magnetic role of O vacancies in ZnO. RT ferromagnetism and the anomalous Hall effect (AHE) were observed in the ZnO film prepared under high vacuum and substrate temperature (T_s) of RT, confirming the ferromagnetic contributions from O vacancies mostly locating at the grain boundaries.

2. Experimental details

ZnO films were prepared on surface oxidized Si substrates by pulsed laser deposition (PLD) from analytically pure ZnO targets using a KrF excimer laser. The film thickness was controlled by the number of laser pulses (5000 in this paper) with pulse energy of 300 mJ and ex situ determined by scanning electron microscope (SEM, FEI Quanta200). The highest vacuum in our system was up to 1.5×10^{-7} Pa. It must be noted that contacting any metal has been avoided. We inserted another Si substrate between the sample and holder. We used plastic tweezers and paid much attention to avoid any contamination. In this paper, we present the results of three ZnO films. ZnO-a (210 nm thick) was prepared under high vacuum and T_s of 500 °C, ZnO-b (210 nm thick) under high vacuum and T_s of RT, and ZnO-c (270 nm thick) under O_2 pressure of 10 Pa and T_s of 500 °C. The structures of the films were studied by X-ray diffraction (XRD, Rigaku UltimaIII) with Cu Kα radiation, X-ray photoelectron spectroscopy (XPS, ThermoFisher SCIENTIFIC) with an Al Kα X-ray source ($h\nu=1486.6$ eV) at a base pressure of 1×10^{-5} Pa in the analysis chamber and the film surface was etched by Ar^+ sputtering, and

* Corresponding author.
E-mail address: xuqingyu@seu.edu.cn (Q. Xu).

0921-4526/$ - see front matter © 2010 Elsevier B.V. All rights reserved.
doi:10.1016/j.physb.2010.09.045

scanning probe microscope (SPM, Veeco Nanoscope Dimension V) at room temperature. The photoluminescence (PL) spectra of the samples were acquired at room temperature with acquisition time of 0.1 s by excitation with the 500 nm line of a Xe lamp (Horiba Jobin Yvon Fluorolog-3). The magnetization and electrical transport (magnetoresistance (MR) and Hall) with standard six-probe method were measured by a physical property measurement system (PPMS-9, Quantum Design).

3. Results and discussions

Fig. 1 shows the X-ray diffraction (XRD) spectra of these films. As can be clearly seen that only the ZnO (0 0 2) peak can be observed except for the (4 0 0) peak from the (1 0 0) Si substrates, indicating the highly (0 0 2) texture of ZnO films on the surface oxidized Si substrates without any impurity phases. The substrate temperature has significant influence on the grains size. As can be seen, the ZnO-c film shows the narrowest (0 0 2) peak. Though ZnO-a was prepared under the same substrate temperature as ZnO-c films; however, the (0 0 2) peak of ZnO-a is broader than that of ZnO-c, indicating the O_2 pressure influences the film growth. Using the Scherrer equation, we calculated the grain size for ZnO films: 14 nm for ZnO-a, 6 nm for ZnO-b, and 33 nm for ZnO-c. The surface roughness obtained by SPM is 0.803 nm for ZnO-a, 0.313 nm for ZnO-b, and 3.04 nm for ZnO-c.

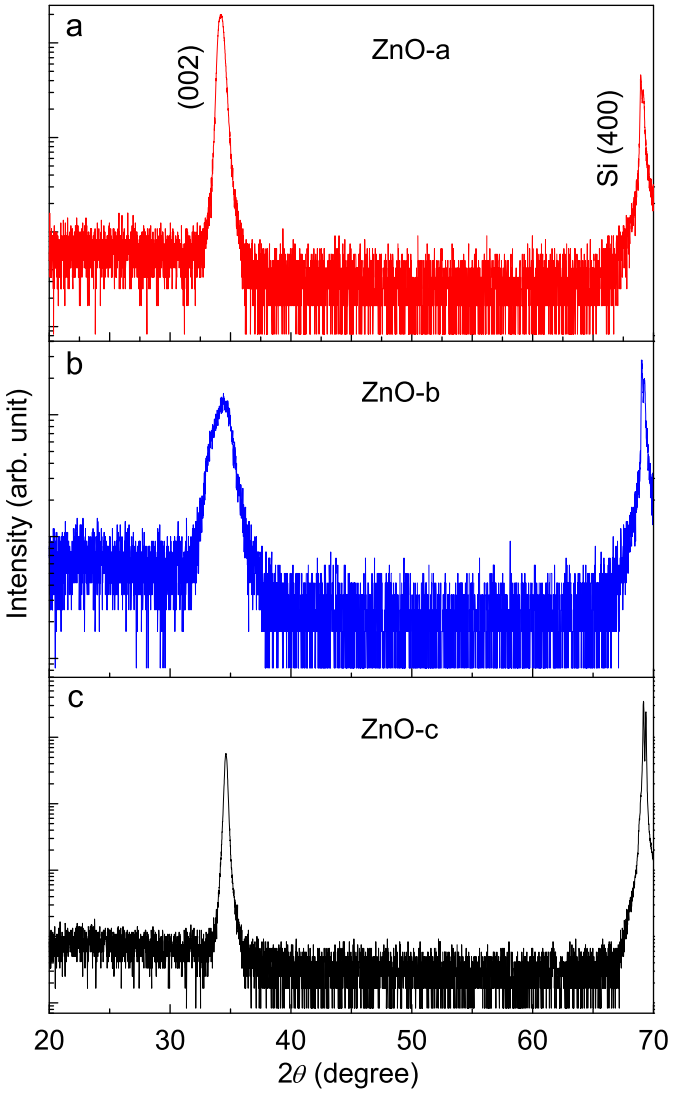

Fig. 1. XRD patterns of ZnO-a, ZnO-b, and ZnO-c films.

To further confirm the purity of the ZnO films, XPS was used for the elemental analysis. Fig. 2 shows the XPS survey spectrum of ZnO-b film for the binding energy range 0 and 1150 eV. It must be noted that similar spectra were observed for ZnO-a and ZnO-c films. Except for the C1s peak from contaminations due to hydrocarbon adsorption on sample surface from the laboratory environment, the spectrum contains all the major core lines of Zn and O, as well as the Zn(LMM) Auger transition lines [13,14]. The XPS survey spectra clearly indicate that no impurity elements were included in the ZnO films.

The magnetic properties of the ZnO films were studied at RT. For ZnO-c film, only linear *M–H* curve with negative slope was observed, indicating a diamagnetic property. ZnO-a exhibits very weak ferromagnetism while clear ferromagnetic hysteresis is observed in ZnO-b (Fig. 3(a)). The diamagnetic signal may come from the Si substrate and ZnO matrix. Fig. 3(b) shows the *M–H*

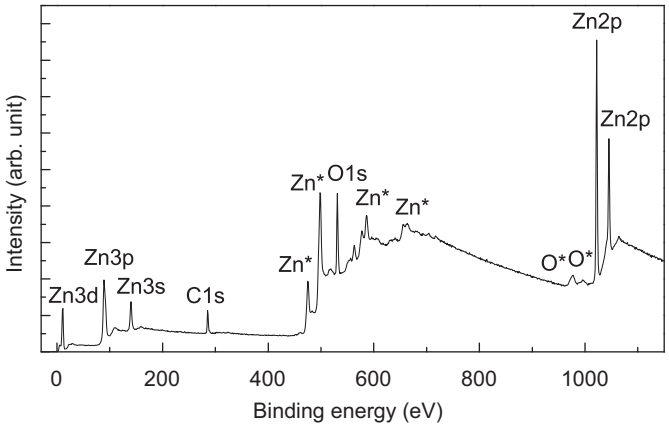

Fig. 2. XPS survey spectrum of ZnO-b film for the binding energy range 0–1150 eV. Similar spectra were observed for ZnO-a and ZnO-c films.

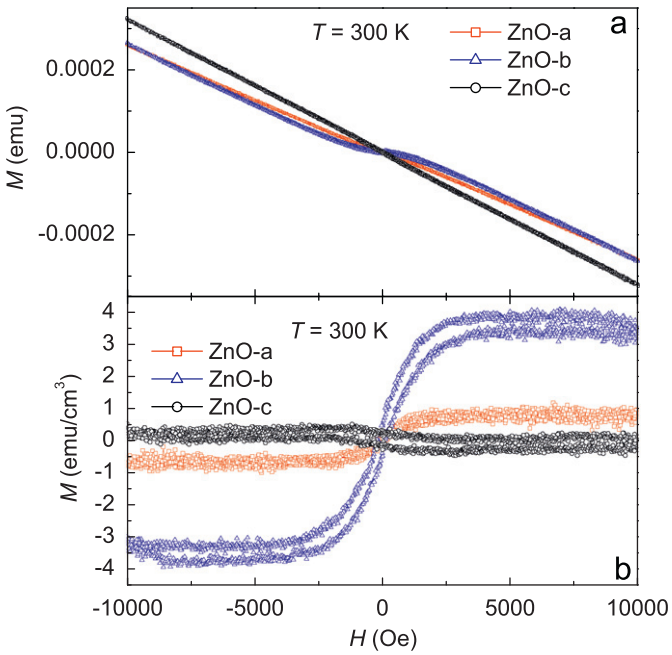

Fig. 3. (a) The raw data of *M–H* curves, and (b) *M–H* curves after subtracting the high field linear diamagnetic background, for ZnO-a, ZnO-b and ZnO-c films measured at 300 K.

curves for ZnO-a, ZnO-b, and ZnO-c films measured at 300 K after subtracting the high field linear diamagnetic background. ZnO-b film exhibits clear hysteresis loop, with saturation magnetization (M_s) of about 3.5 emu/cm^3. For ZnO-a film, weak ferromagnetism can also be observed with M_s of about 0.8 emu/cm^3. For ZnO-c film, the negative slope around zero field might be due to the different diamagnetic susceptibility of ZnO and Si.

As the magnetization measurement is a bulk effect, the ferromagnetic contributions from the contaminations and small concentration of impurities below detecting limits of XRD and XPS cannot be excluded. To confirm the intrinsic nature of the observed ferromagnetism in ZnO-b film, we performed the magnetotransport measurements, since the current will only pass through the conductive film on the highly insulating Si substrates covered by insulator SiO_2. As shown in Fig. 4(a), positive MR was observed at 5 K. The MR is defined as $[R(H)-R(0)]\times 100\%/R(0)$. At 20,000 Oe, MR is about 1%. Positive MR was general observed in 3d TM doped ZnO at low temperature, which was attributed to the quantum correction on the conductivity due to the s–d exchange interaction induced spin splitting of the conduction band [15–17]. At 300 K, negligible small negative MR was observed below 10,000 Oe, and then positive MR was observed with further increasing field.

Fig. 4(b) shows the temperature dependent resistivity ρ. ρ increases drastically with decrease in temperature from 0.017 Ω cm at 350 K to 4.28 Ω cm at 5 K, indicating the typical semiconductor behavior. Recently, Chou et al. [18] studied the spin current in Co-doped ZnO, and classified the electrons into two categories. One is the electrons in the conduction band, which can be described by the thermal excitation model, $\rho\sim\exp(E_d/kT)$, where E_d is the activation energy, k the Botzmann constant, and T the temperature. The other is the electrons hopping within discrete localized states, which can be described by the variable range hopping, $\rho\sim\exp[(C/T)^{1/4}]$, where C is the constant associated with the localized radius and the hopping radius of carriers around localized states. As can be seen in the inset of Fig. 4(b), ln ρ has nonlinear relationship with $1/T$ in almost the whole temperature range, but is nearly linear in dependence on the $1/T^{1/4}$, especially below 200 K. This indicates that the conducting electrons in ZnO-b film mainly hop within discrete localized states and are spin polarized, and the magnetic coupling can be interpreted to be mediated by these spin polarized electrons.

The general criteria for the intrinsic ferromagnetism is the observation of AHE. Fig. 5 shows the magnetic field dependent Hall resistivity ρ_{xy} at 5 and 300 K. The curve is very noisy at 5 K, which is due to the too large resistance at 5 K. The Hall resistivity ρ_{xy} is known to be a sum of ordinary and anomalous Hall terms, $\rho_{xy}=R_0B+R_s\mu_0M$, where B is the magnetic induction, μ_0 the magnetic permeability, M the magnetization, R_0 the ordinary Hall coefficient, and R_s the anomalous Hall coefficient. The first is the ordinary Hall effect (OHE), linear in B, and the second is the AHE proportional to M [19]. As AHE is always much larger than OHE, the Hall curve is similar to the shape of the magnetization curve. For comparison, the M–H curves at 5 and 300 K are also shown in

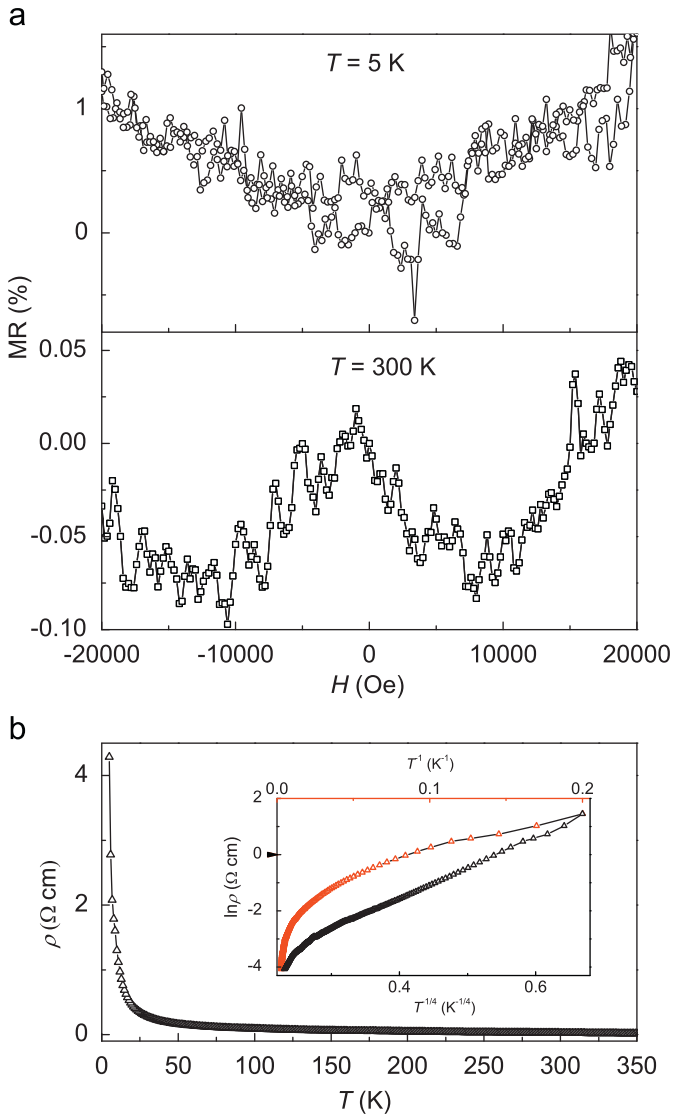

Fig. 4. (a) field dependent MR measured at 5 and 300 K for ZnO-b film, (b) temperature dependent resistivity for ZnO-b film, the inset shows the ln ρ in dependence on T^{-1} and $T^{-1/4}$.

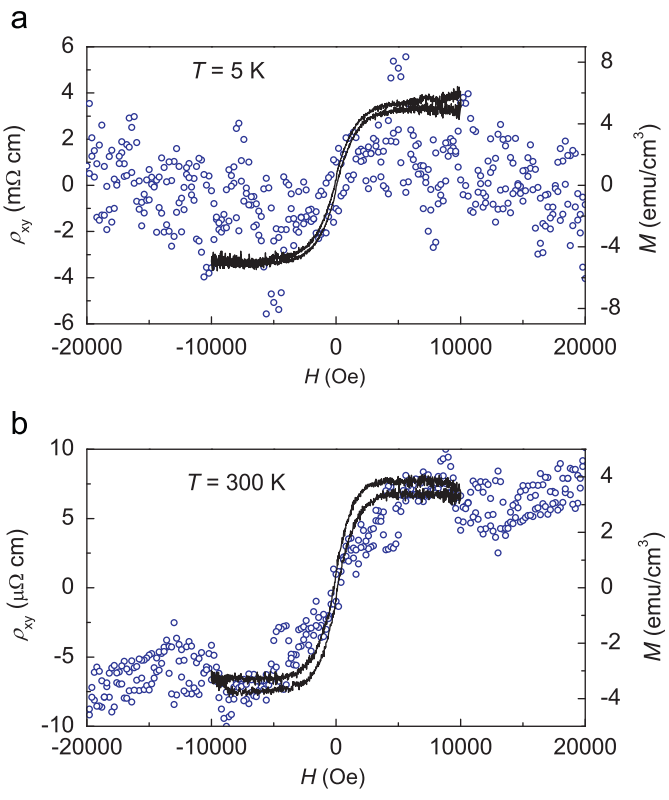

Fig. 5. Field dependent Hall resistivity for ZnO-b film at (a) 5 and (b) 300 K (open circle). The corresponding M–H curves are also shown (solid curves).

Fig. 5(a) and (b), respectively. It can be seen that the ρ_{xy}–H curves coincide with the M–H curves quite well. The slight discrepancy might be due to the different field orientation between the magnetization measurement (field in the film plane) and the Hall measurement (field perpendicular to the film plane). The negative slope in the high field part of the Hall curve at 5 K indicates the n-type conductivity of ZnO-b film, and the electron concentration and mobility can be evaluated to be about 3.7×10^{17} cm^{-3} and 3.9 cm^{2}V^{-1}s^{-1}, respectively. The clear observation of the AHE indicates the intrinsic ferromagnetism in ZnO-b film.

Clear ferromagnetism has been observed in ZnO-b film and weak ferromagnetism in ZnO-a film, while diamagnetism in ZnO-c film. The main preparation parameter difference between these films is the O_2 pressure during film preparation, high vacuum for ZnO-a and ZnO-b while 10 Pa O_2 for ZnO-c. It is reasonable to assume that the ZnO-c film was fully oxidized with less O vacancies but ZnO-a and ZnO-b films were partially oxidized with more O vacancies. To confirm this, we performed the PL measurements on these three films. As has been suggested, the green emission peak centered at around 520 nm can be attributed to the transition between the photoexcited holes and singly ionized O vacancy [20]. The PL spectra of these three films are shown in Fig. 6. The green emission peak at about 520 nm is only clearly observed in ZnO-b film, indicating the large numbers of O vacancies in the ZnO-b film.

Another factor to be clarified is the chemical state of Zn under different O_2 pressure and T_s. Generally the C1s peak from contaminations was used to calibrate the XPS spectra [13]. However, as the spectra were taken after the Ar^+ etching of the film surface, the C1s peak is very weak and cannot be used for the calibration. Here we use the O1s peak for the calibration. As the O in ZnO film has two states, O_l the lattice oxygen and O_a the oxygen in air, which is absorbed by the surface of ZnO films [13]. After etching the film surface, only the peak from O_l can be clearly observed. Fig. 7 shows the XPS spectra of Zn2p for these three ZnO films after the calibration. The peak position of Zn2p for ZnO-a is 1021.75 eV, 1021.68 eV for ZnO-b, and 1021.70 eV for ZnO-c. Taking into account the energy resolution of ±0.1 eV, the shift of Zn2p peaks to lower side is very small in magnitude. However, this aspect cannot be ruled out by our present studies, especially when our XPS data does show a small shift in Zn2p peaks when the O deficiency is maximum in ZnO-b. This should be attributed to at least some small change in Zn chemical state by electronic charge transfer upon O vacancy creation, in order to maintain the electronic charge balance, which is supported by the recent reports that the cation peak shifts to lower energy with increase in O vacancy concentration [21,22]. The shifts would be more reliable, significant, and quantitative, had we calibrated the peaks with C1s line, which we could not do for the reason stated above. We suggest that the O vacancies might mainly locate at the grain boundaries, as suggested by the recent study of Singhal et al. [22] that grain boundaries are created with increase in O vacancy concentration, which needs further structural characterizations in the future. It has been pointed out by Straumal et al. [23] that the ratio of the grain boundary area to the grain volume exceeds a certain threshold value and the related vacancies are the intrinsic origin for RT ferromagnetism. The ZnO-b film has the smallest grain size, thus the largest grain boundary area, leading to the highest concentration of O vacancies and strongest ferromagnetism at RT. Our results presented here clearly demonstrate that the high concentration of O vacancies is the key origin for the observed ferromagnetism in pure ZnO.

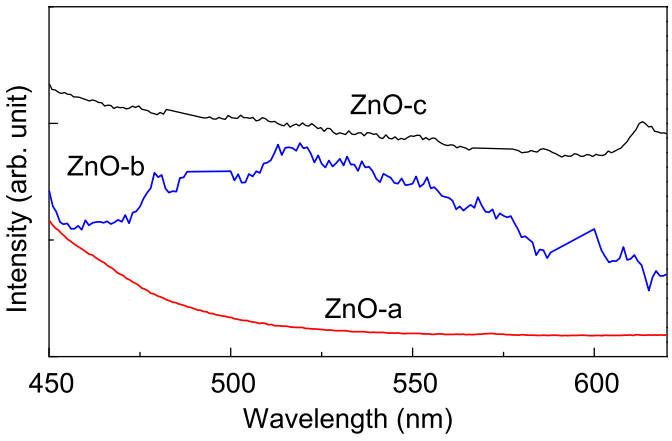

Fig. 6. PL spectra of ZnO-a, ZnO-b, and ZnO-c films measured at room temperature. A broad peak can be observed at around 520 nm for ZnO-b film.

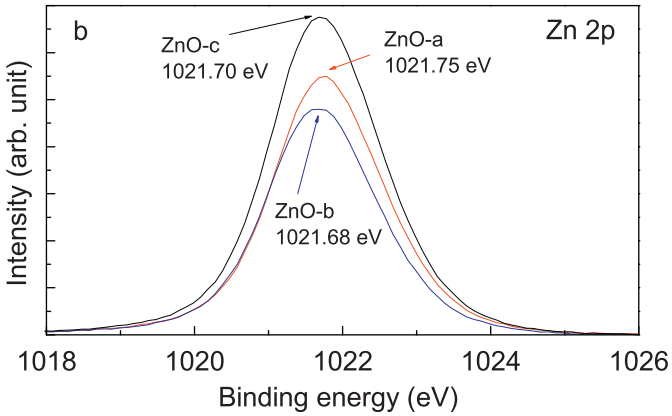

Fig. 7. XPS spectra of Zn2p for ZnO-a, ZnO-b, and ZnO-c films.

4. Conclusions

In conclusion, we prepared pure ZnO films on oxidized Si substrates under different O_2 pressure and substrate temperature. The ZnO film prepared under high vacuum (1.5×10^{-7} Pa) and substrate temperature of RT exhibits clear RT ferromagnetism, and the intrinsic nature was confirmed by the observation of AHE. The PL spectra shows the high concentration of O vacancies in the RT ferromagnetic pure ZnO film while the O vacancies cannot be resolved in other ZnO films. The high concentration of O vacancies is mediated by the spin polarized electrons hopping between discrete states, inducing the RT ferromagnetism in ZnO films.

Acknowledgements

This work is supported by the National Natural Science Foundation of China (50802041, 50872050), National Key Projects for Basic Researches of China (2005CB623605, 2009CB929503, 2010CB923404), by NCET-09-0296 and Southeast University. M. X. Xu acknowledges the support from the Research Fund for the Doctoral Program of Higher Education of China (Grant no. 20070286037).

References

[1] J. Fabian, A. Matos-Abiague, C. Ertler, P. Stano, I. Žutić, Acta Phys. Slovaca 57 (2007) 565.
[2] I. Žutić, J. Fabian, S. Das Sarma, Rev. Mod. Phys. 76 (2004) 323.
[3] T. Dietl, H. Ohno, F. Matsukura, J. Cibert, D. Ferrand, Science 287 (2000) 1019.

[4] Q. Xu, H. Schmidt, S. Zhou, K. Potzger, M. Helm, H. Hochmuth, M. Lorenz, A. Setzer, P. Esquinazi, C. Meinecke, M. Grundmann, Appl. Phys. Lett. 92 (2008) 082508.
[5] M. Khalid, M. Ziese, A. Setzer, P. Esquinazi, M. Lorenz, H. Hochmuth, M. Grundmann, D. Spemann, T. Butz, G. Brauer, W. Anwand, G. Fischer, W.A. Adeagbo, W. Hergert, A. Ernst, Phys. Rev. B 80 (2009) 035331.
[6] S. Banerjee, M. Mandal, N. Gayathri, M. Sardar, Appl. Phys. Lett. 91 (2007) 182501.
[7] G. Xing, D. Wang, J. Yi, L. Yang, M. Gao, M. He, J. Yang, J. Ding, T.C. Sum, T. Wu, Appl. Phys. Lett. 96 (2010) 112511.
[8] A. Sundaresan, R. Bhargavi, N. Rangarajan, U. Siddesh, C.N.R. Rao, Phys. Rev. B 74 (2006) 161306R.
[9] N.H. Hong, J. Sakai, V. Brizé, J. Phys.: Condens. Matter 19 (2007) 036219.
[10] J.B. Yi, H. Pan, J.Y. Lin, J. Ding, Y.P. Feng, S. Thongmee, T. Liu, H. Gong, L. Wang, Adv. Mater. 20 (2008) 1170.
[11] X. Zuo, S. Yoon, A. Yang, W. Duan, C. Vittoria, V.G. Harris, J. Appl. Phys. 105 (2009) 07C508.
[12] Q. Wang, Q. Sun, G. Chen, Y. Kawazoe, P. Jena, Phys. Rev. B 77 (2008) 205411.
[13] L. Wei, Z. Li, W.F. Zhang, Appl. Surf. Sci. 255 (2009) 4992.
[14] A. Nayak, H.D. Banerjee, Appl. Surf. Sci. 148 (1999) 205.
[15] T. Andrearczyk, J. Jaroszyński, G. Grabecki, T. Dietl, T. Fukumura, M. Kawasaki, Phys. Rev. B 72 (2005) 121309 R.
[16] Q. Xu, L. Hartmann, H. Schmidt, H. Hochmuth, M. Lorenz, R. Schmidt-Grund, C. Sturm, D. Spemann, M. Grundmann, Phys. Rev. B 73 (2006) 205342.
[17] Q. Xu, L. Hartmann, H. Schmidt, H. Hochmuth, M. Lorenz, D. Spemann, M. Grundmann, Phys. Rev. B 76 (2007) 134417.
[18] H. Chou, C.P. Lin, H.S. Hsu, S.J. Sun, Appl. Phys. Lett. 96 (2010) 092503.
[19] J.S. Higgins, S.R. Shinde, S.B. Ogale, T. Venkatesan, R.L. Greene, Phys. Rev. B 69 (2004) 073201.
[20] Y. Yang, J. Qi, W. Guo, Z. Qin, Y. Zhang, Appl. Phys. Lett. 96 (2010) 093107.
[21] A. Samariya, R.K. Singhal, S. Kumar, Y.T. Xing, S.C. Sharma, P. Kumari, D.C. Jain, S.N. Dolia, U.P. Deshpande, T. Shripathi, E. Saitovitch, Appl. Surf. Sci 257 (2010) 585.
[22] R.K. Singhal, A. Samariya, S. Kumar, Y.T. Xing, D.C. Jain, S.N. Dolia, U.P. Deshpande, T. Shripathi, E.B. Saitovitch, J. Appl. Phys. 107 (2010) 113916.
[23] B.B. Straumal, A.A. Mazilkin, S.G. Protasova, A.A. Myatiev, P.B. Straumal, G. Schütz, P.A. van Aken, E. Goering, B. Baretzky, Phys. Rev. B 79 (2009) 205206.